Chinese Herbal Medicines 17 (2025) 368–379

Contents lists available at ScienceDirect

Chinese Herbal Medicines

journal homepage: www.elsevier.com/locate/chmed

Original Article

Osthole ameliorates chronic pruritus in 2,4-dichloronitrobenzene-induced atopic dermatitis by inhibiting IL-31 production

Shuang He [a,b,c], Xiaoling Liang [a,b,c], Weixiong Chen [d,e], Yangji Nima [a], Yi Li [a], Zihui Gu [a], Siyue Lai [a], Fei Zhong [a], Caixiong Qiu [a,b,c], Yuying Mo [f], Jiajun Tang [f], Guanyi Wu [a,b,c,*]

[a] School of Basic Medicine, Guangxi University of Chinese Medicine, Nanning 530299, China
[b] Key Laboratory of Characteristic Experimental Animal Models of Guangxi, Nanning 530299, China
[c] Guangxi Key Laboratory of Translational Medicine for Treating High-Incidence Infectious Diseases with Integrative Medicine, Nanning 530299, China
[d] School of Health Science and Engineering, University of Shanghai for Science and Technology, Shanghai 200093, China
[e] Faculty of Chinese Medicine Science, Guangxi University of Chinese Medicine, Nanning 530299, China
[f] School of Pharmacy, Guangxi University of Chinese Medicine, Nanning 530299, China

ARTICLE INFO

Article history:
Received 1 September 2023
Revised 31 October 2023
Accepted 4 January 2024
Available online 9 April 2024

Keywords:
atopic dermatitis
chronic pruritus
Cnidium monnieri (L.) Cusson
IL-31
NF-κB
osthole
PPAR

ABSTRACT

Objective: This study aims to elucidate the therapeutic potential of osthole for the treatment of atopic dermatitis (AD), focusing on its ability to alleviate chronic pruritus (CP) and the underlying molecular mechanisms.

Methods: In this study, we investigated the anti-inflammatory effects of osthole in both a 2,4-dichloronitrobenzene (DNCB)-induced AD mouse model and tumor necrosis factor-α (TNF-α) and interferon-γ (IFN-γ) stimulated human immortalized epidermal (HaCaT) cells. The anti-itch effect of osthole was specifically assessed in the AD mouse model. Using methods such as hematoxylin and eosin (HE) staining, enzyme-linked immunosorbent assay (ELISA), western blot (WB), quantitative real-time PCR (qRT-PCR), and immunofluorescence staining.

Results: Osthole improved skin damage and clinical dermatitis scores, reduced scratching bouts, and decreased epidermal thickness AD-like mice. It also reduced the levels of interleukin (IL)-31 and IL-31 receptor A (IL-31 RA) in both skin tissues and HaCaT cells. Furthermore, Osthole suppressed the protein expression levels of phosphor-p65 (p-p65) and phosphor-inhibitor of nuclear factor kappa-Bα (p-IκBα). Meanwhile, it increased the protein expression levels of peroxisome proliferator-activated receptor α (PPARα) and PPARγ in HaCaT cells.

Conclusion: These findings indicated that osthole effectively inhibited CP in AD by activating PPARα, PPARγ, repressing the NF-κB signaling pathway, as well as the expression of IL-31 and IL-31 RA.

1. Introduction

Atopic dermatitis (AD) is a persistent and recurring inflammatory skin condition characterized by chronic eczema-like lesions, dry skin, and intense pruritus. Pruritus, an unpleasant and irritating sensation that triggers the urge to scratch, can be categorized as either acute (lasting for ≤ 6 weeks) or chronic (lasting for more than six weeks), depending on its duration (Xia, Li, & Chen, 2022). The most prominent symptom of AD is chronic pruritus (CP), which is usually severe, recurrent, and widespread. CP can trigger a cycle of scratching and more itching (Frazier & Bhardwaj, 2020), leading to sleep disturbances, decreased quality of life, anxiety, depression, and an increased risk of suicidal behavior in affected individuals (Tang & Yao, 2022). The occurrence of AD is evident across all age groups and exhibits a rising trend in recent years (Hu, 2021). Over the last three years, an epidemiological survey reveals that the prevalence of AD among adults ranges from 7% to 10%. Likewise, the incidence rate of AD among children globally is estimated to be between 15% and 20% (Li, Heng, & Wang, 2022).

For individuals with mild to moderate AD, CP is the most distressing symptom. Whereas, in cases where the skin lesions are large and there is extensive exudation, CP becomes an even greater burden for patients (Silverberg et al., 2018). The intricate process of CP is intricately linked to various factors such as neural pathways, immune system regulation, skin barrier function, the presence of itch-inducing agents and their corresponding receptors, as well as external environmental factors (Hu, 2021). An imbalance in T

* Corresponding author.
E-mail address: wugy@gxtcmu.edu.cn (G. Wu).

https://doi.org/10.1016/j.chmed.2024.01.003
1674-6384/

helper (Th) 1/Th2 cell differentiation can lead to abnormal cytokines secretion, which is a crucial immunological mechanism in the development of AD. Th2 cytokines, including interleukin (IL)-4, IL-13, and IL-31, are implicated in both the initiation of inflammatory responses in AD and the perpetuation of CP (Jiang & Wang, 2016).

IL-31, belonging to the IL-6 interleukin family, is chiefly generated by Th2 cells and elicits various effects on both the skin and the immune system. Its roles encompass skin barrier reconstruction, facilitation of nerve growth, provocation of itch sensation, and modulation of intercellular communication within the skin (Dou et al., 2018). The severity of CP in adult and adolescent AD patients is directly related to the levels of IL-31 (Duca, Sur, Armat, Samasca, & Sur, 2022). Prolonged pruritus induction, lasting over 1.5 s, can be attributed to the direct effect of IL-31, which does not impact the expression of IL-31 receptor A (IL-31 RA) (Cornelissen et al., 2012). Nevertheless, repeated subcutaneous administration of IL-31 for multiple days can elevate itchiness in mice, as well as upregulate the expression of IL-31 RA in dorsal root ganglion (DRG) neurons (Cevikbas et al., 2014). The formation of functional receptor complexes, essential for IL-31 signaling, occurs through the pairing of IL-31 RA with oncostatin-M receptor β (OSMRβ), thus facilitating the signaling process. Moreover, IL-31 has the potential to induce the secretion of several cytokines, including IL-17A, C-X-C motif chemokine ligand 10 (CXCL10), and matrix metalloproteinase-9, from keratinocytes through the upregulation of natriuretic peptide precursor B gene expression in the peripheral DRG and skin. This process facilitates the synthesis and release of brain natriuretic peptide. The direct activation of keratinocytes triggers the secretion of thromboxane and leukotriene B4. Ultimately, the activation of IL-31 can lead to an itching sensation through the promotion of C—C chemokine ligand 20 (CCL20) release from dendritic cells, the facilitation of DRG neuron growth, and the increase in nerve fiber density (Li, Qiu, He, Huang, & Wu, 2022). At present, the management of AD primarily centers on mitigating or eradicating observable manifestations. Nevertheless, extended utilization of typical medications like glucocorticoids, phosphodiesterase 4 inhibitors, and oral antihistamines may result in adverse reactions such as skin thinning, bruising, and dilated blood vessels (Wang, 2020). Consequently, the primary focus of current research is to identify therapeutic medications that exhibit high efficacy and minimal adverse reactions.

Cnidii Fructus (Shechuangzi in Chinese), the dried ripe fruits of *Cnidium monnieri* (L.) Cusson (Fig. 1A), holds a longstanding position in traditional Chinese medicine (TCM). This herb is recognized for its pungent, bitter taste, and warming properties. Within modern TCM, it is extensively utilized to address persistent skin pruritus, superficial fungal infections, as well as various dermatoses like scrotal eczema and scabies (Qin, Hu, Zhang, & Mao, 2018). Yu et al. discovered that the total coumarins from *Cnidii Fructus* significantly inhibit AD-like symptoms in rats induced by 2,4-dichloronitrobenzene (DNCB), including the suppression of pruritus triggered by IL-31, thymic stromal lymphopoietin (TSLP), and histamine (Yu, Deng, Wang, Sun, & Xu, 2021). In a separate study, it was demonstrated that the ethyl acetate extract from *Cnidii Fructus* effectively alleviated DNFB-induced AD-like symptoms in C57BL/6 mice, as evidenced by reduced epidermal hyperplasia, mast cell infiltration, and mitigation of chronic or acute scratching behavior (Chen et al., 2020). Due to its high concentration of coumarins, osthole (Fig. 1B), a component extracted from *Cnidii Fructus*, was found to possess an extensive variety of pharmacological effects, including an antiallergic (Kordulewska, Topa, Stryiński, & Jarmołowska, 2021), anti-inflammatory (Meng et al., 2018), antispasmodic (Sadraei, Shokoohinia, Sajjadi, & Ghadirian, 2012), antihyperlipidemia (Wu et al., 2020), and immunomodulatory (Kordulewska et al., 2021) effects. Previous research has demonstrated its ability to restore the skin barrier (Ashrafizadeh et al., 2020) and relieve itching by directly inhibiting the production of thymic stromal lymphopoietin (TSLP) (Fu & Hong, 2019) and activating transient receptor potential vanilloid 1 (TRPV1) in DRG neurons (Yang et al., 2021b). Nevertheless, the potential therapeutic effects of osthole through IL-31 and the mechanism of its action remain to be further explored.

Keratinocytes play a crucial role in regulating skin inflammation by responding to a variety of external and internal signals, releasing a spectrum of cytokines and chemokines upon stimulation (Guilloteau et al., 2010). In the context of AD, the complex interaction among keratinocytes, immune cells and nerves significantly influences both the development and symptoms of the condition (Yang et al., 2021a). Specifically in AD, keratinocytes play a significant role by producing pro-inflammatory cytokines, contributing to the development of inflammatory skin lesions (Lee et al., 2020). This emphasizes the substantial therapeutic potential of compounds that can regulate keratinocyte function. This study employed a human immortalized epidermal (HaCaT) cell line model stimulated by tumor necrosis factor-α (TNF-α)/interferon-γ (IFN-γ) (Oh et al., 2022) and a C57BL/6J mouse model exposed to DNCB to assess the effectiveness of osthole in managing CP associated with AD. Our research revealed that osthole could successfully ameliorate CP in AD through the activation of peroxisome proliferators-activated receptor α (PPARα) and PPARγ, and the inhibition of nuclear factor kappa-B (NF-κB) signaling pathway and the expression of IL-31 and IL-31 RA.

2. Materials and methods

2.1. Reagents

Osthole, with a purity of ≥ 99%, was obtained from Aladdin (Shanghai, China) and stored at 4 °C. It is a pure drug monomer, distinct from the extract of *C. monnieri*. For *in vivo* and *in vitro* experiments, osthole was dissolved in dimethyl sulfoxide (DMSO) (10%) at a concentration of 50 mg/kg and then diluted according to each experimental condition. DNCB was obtained from Aldrich (Shanghai, China). 1% and 0.5% DNCB was dissolved in an acetone: olive oil mixture (4:1 vol/vol). Tacrolimus was obtained from Astellas (Beijing, China).

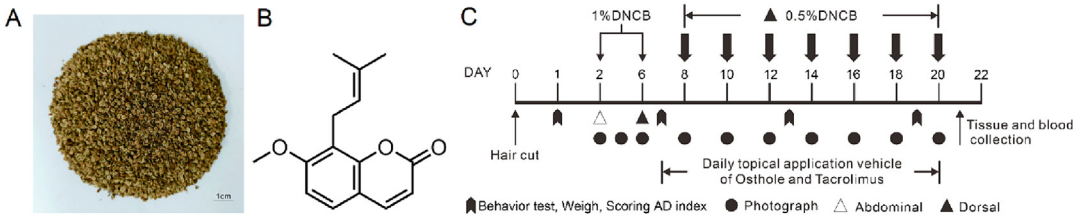

Fig. 1. Materials and experimental scheme. (A) Apperance of *Cnidii Fructus*. (B) Chemical structure of osthole. (C) Experimental scheme.

2.2. Animals and grouping

The male C57BL/6J mice (8-week-old) were purchased from the Hunan Slake Jingda Experimental Animal Co., Ltd. [Changsha, China) (SCXK (Xiang) 2019-0004]. The mice were fed with standard laboratory chow and water ad libitum and housed in a temperature (23 ± 2) °C and light-controlled room under a 12 h light/dark cycle with a relative humidity of (55 ± 15)%. All experiment protocols were approved by the Institutional Animal Care and Use Committee of Guangxi University of Chinese Medicine (Ethics license DW20181220-153) and were carried out according to relevant guidelines and regulations.

The C57BL/6J mice were divided into seven groups: (1) control, (2) DNCB sensitization only (J. Lee, Ki, Kim, & Lee, 2018), (3) DNCB + DMSO, (4) DNCB + osthole 5 mg/kg, (5) DNCB + osthole 25 mg/kg, (6) DNCB + osthole 50 mg/kg (Fu & Hong, 2019) and (7) DNCB + topical tacrolimus 0.03% (Barequet et al., 2013). Cutaneous DNCB sensitization was performed by applying 1% DNCB on the dorsal skin of the mice at day 2 and day 6. To induce AD-like symptoms, 0.5% DNCB was topically applied on the mice every other day for two weeks (day 8 to 20) in groups 2−7. Tacrolimus was topically applied to the mouse dorsal skin of group 7 daily for two weeks (day 7 to 20) (Fig. 1C). The weight, dermatitis score and scratching behavior were measured, the lesions were photographed, and mice were sacrificed for tissue analysis and sera diagnosis at day 21.

2.3. Evaluation of skin conditions and itch

Skin conditions which defined as erythema, edema, dry skin or desquamation, were observed macroscopically and evaluated according to their severity. The scores were defined within a range of 0 to 3 according to the following criteria: a score of 0 means no symptoms, 1 indicates mild symptoms, 2 reflects severe symptoms, and 3 signifies significant severity. There are three experimenters giving independently scores, and the total score of skin conditions is defined as the sum of the individual scores indicated above. Itch was evaluated by measuring the accumulated scratching time during one-hour observation period.

2.4. Histopathological analysis

Skin tissues from each mouse were filled with 4% paraformaldehyde and immersion fixed for 16 h at 4 °C. Tissues were dehydrated, embedded in paraffin and sectioned at 5 μm. The sections were stained with hematoxylin and eosin (H&E) to observe epidermal thickness. Images were captured under an optical microscope, and then assembled using CorelDRAW 2019. Epidermal thickness was defined as the distance from the epidermal-dermal junction up to the stratum corneum. Thickness measurements were obtained using Image J software.

2.5. Enzyme-linked immunosorbent assay (ELISA)

The serum levels of Immunoglobulin E (IgE), TNF-α, IL-6, histamine and IL-31 were quantified using commercial ELISA kits (Bioswamp, Wuhan, China), in accordance with the manufacturer's instructions.

2.6. Cell culture and viability assay

HaCaT cells were cultured in Eagle's MEM medium with 10% fetal bovine serum (FBS) at 37 °C in 5% CO_2. The viability of HaCaT cells was measured by using 3-(4,5-dimethylthiazol-2-y1)-2,5-di phenyltetrazolium bromide (MTT) assay. Cells were seeded at 5×10^4 cells/well of 96-well plates overnight and then treated with various concentrations of osthole (0.1, 0.3, 1, 3, 10, 30 μmol/L) for 24 h in a 37 °C incubator. Adding MTT reagents to each well, and the plate was incubated for a further 4 h. Removing the supernatant, the crystallized formazan was dissolved in DMSO. Absorbance at 550 nm was measured using a Microplate Reader.

2.7. Western blot (WB) analysis

After the HaCaT cells grew to 90% full, they were digested and seeded into 6-well plates at a density of 1.2×10^6 cells per well. Following overnight incubation to allow for cell attachment, the cells were pretreated with osthole for 24 h and subsequently stimulated with TNF-α and IFN-γ for 2 h. The medium in the 6-well plates was then aspirated, and the cells were washed three times with phosphate buffer solution (PBS) buffer before the final aspiration. A mixture of radioimmunoprecipitation assay (RIPA) lysis buffer (Beyotime, Shanghai, China), protease inhibitor, and phosphatase inhibitor in a ratio of 100:1:1 was added to each well, using 1 mL per well, and the plates were shaken thoroughly before being placed on ice for 15 min to lyse the cells. The lysed cell solution was then collected into sterile 1.5 mL eppendorf (EP) tubes. Each tube was subjected to ultrasonic disruption for 1 min, repeated three times. Following sonication, the HaCaT cell lysates were centrifuged at 12 000 r/min for 5 min at 4 °C to pellet the cellular debris and remove the supernatant. Subsequently, the protein concentration was quantified using a bicinchoninic acid (BCA) protein assay kit (Beyotime, Shanghai, China). Additionally, for the mouse skin tissue samples, a small amount of minced dorsal skin tissue was placed in a 2 mL EP tube, and steel beads and 200 μL of lysis buffer were added for complete homogenization. After thorough lysis on ice for 30 min, the samples were centrifuged, and the supernatant was collected. Protein concentration was determined, and subsequent denaturation steps were performed. The lysates were then separated by electrophoresis and transferred onto polyvinylidene difluoride (PVDF) membranes. The membranes were then blocked with confining liquid and incubated overnight at 4 °C with respective primary antibodies. After washing, the membranes were incubated with secondary antibodies for 1 h. The proteins were visualized with Gel Imaging System (Shenhua Science Technology, Hangzhou, China) and quantified using the ImageJ software.

2.8. Quantitative real-time polymerase chain reaction (RT-qPCR)

Using trizol to extract RNA from dorsal skin and HaCaT cells, then using a reverse transcription kit (Vazyme, Nanjing, China) to reverse transcribe RNA into cDNA, the primers of RT-qPCR were shown in Table 1. The PCR amplification condition was initial denaturation at 95 °C for 10 min, followed by 40 cycles of 95 °C for 15 s, 60 °C for 60 s, 95 °C for 15 s and 1 cycle of 60 °C for 60 s, 95 °C for 15 s. Relative mRNA expression levels were analyzed three times and normalized to the internal control gene, *β-actin*.

Table 1
Primer sequences.

Genes	Primers	Sequences (5′−3′)	PCR products
β-actin	Forward	CACGATGGAGGGGCCGGACTCATC	240 bp
	Reverse	TAAAGACCTCTATGCCAACACAGT	
IL-31	Forward	GAACAACGAAGCCTACCCTG	232 bp
	Reverse	GTTAATGCTTCCCGGTCCAG	
IL-31 RA	Forward	CTCCCCTGTGTTGTCCTGAT	111 bp
	Reverse	TGTCCCCAGAGTTTCCAGTC	

2.9. Statistical analysis

GraphPad Prism software 9.0 (GraphPad Prism, San Diego, CA, USA) was used for data statistical analysis. All data are presented as means ± standard error of the mean (SEM), and evaluated using One-way analysis of variance (ANOVA) test. A value of $P < 0.05$ was defined as statistically significant.

3. Results

3.1. Osthole ameliorates DNCB-induced AD-like symptoms in mice

After establishing the model of AD-like lesions in the dorsal region of C57BL/6J mice, we assessed the progression and severity of AD by skin lesions, scores and scratching bouts. During the 21-day experimental period, the skin swelling, erythema, cornification, exudation, and dry skin in the DNCB group gradually worsened (Fig. 2A), and the scores increased moderately. However, the application of osthole, particularly in high doses, significantly decreased the scores (Fig. 2B and C). Repeated application of DNCB to mice induced intensively scratching bouts, while osthole and tacrolimus treatment significantly decreased bouts of scratching (Fig. 2D and E). Furthermore, the body weight changes of mice were measured, but there were no significant changes among any of the groups (Fig. 3A). The spleen is an immune organ that is responsible for regeneration and storage of red blood cells. Chronic inflammation always leads to the enlargement of the spleen (Kim et al., 2021a). Thus, an assessment of osthole's impact on the immune system was carried out by measuring spleen coefficient. The results indicated an increase in the spleen coefficient of the model group (Fig. 3B–D, $P < 0.05$), with no significant difference observed between the osthole-treated groups and the model group.

3.2. Osthole mitigated thickening of epidermis in mice

Repeated DNCB stimulation induces a significant inflammatory response in the skin, characterized by epidermal thickening, inflammation, and increased keratin production, resulting in a substantial increase in epidermal thickness compared to the control group (Yang et al., 2023). H&E staining of skin sections revealed that DNCB-treated mice exhibited excessive epidermal keratinization and a marked increase in epidermal thickness. Conversely, mice with AD that were treated with osthole and tacrolimus showed a notable reduction in epidermal thickness (Fig. 4A). The various concentrations of osthole demonstrated a statistically significant decrease in epidermal thickness, with the high-dose group (50 mg/kg) exhibiting particularly significant improvement (Fig. 4B). This finding suggested that osthole possessed therapeutic properties for alleviating the pathological manifestations of AD.

3.3. Osthole reduced mRNA and protein expression of IL-31 and IL-31 RA in epidermal tissues of mice

IL-31 is a cytokine released by Th2 cells that has been observed to cause severe itching and chronic dermatitis when overexpressed (Meng et al., 2021). This is due to its activation of IL-31 RA in sensory neurons through TRPV1, which directly leads to itching (Cevikbas et al., 2014). To see if the severity of AD in mice is correlated with IL-31 and IL-31 RA, the mRNA (Fig. 5A and B) and protein (Fig. 5C–E) expression levels were examined in the epidermal tissues. Our results revealed that the mRNA and protein expression of IL-31 and IL-31 RA increased significantly in DNCB groups. For another, the mRNA and protein expression levels decreased in osthole treatment in a concentration dependent way, which showed that the alleviation of CP in DNCB-induced mice with AD was related to levels of IL-31 and IL-31 RA.

3.4. Osthole decreased inflammatory mediator levels in serum

An elevation in serum total IgE is a common hallmark of AD (No et al., 2021). The level of IgE was all detected at the end of the experiment on day 21. As shown in Fig. 6A, the IgE level in the DNCB group exhibited an increase compared to that of the control group. Nevertheless, the osthole treatment group lowered the generation of IgE induced by DNCB. To evaluate the effect of osthole on immune response, an analysis of TNF-α and IL-6 levels was performed in mouse serum samples (Fig. 6B and 6C). The results showed that the high osthole concentration notably reduced IL-6 levels, while the moderate concentration primarily downregulated TNF-α levels. As a crucial chemical mediator responsible for inducing itching, histamine has been closely linked to AD itching (Song, Park, Kim, Jang, & Kim, 2022), and there is a strong connection between the release of histamine and the activation of IgE as well as the secretion of inflammatory cytokines (Kim & Kim, 2022). Additionally, IL-31 has also emerged as a significant contributor to this condition. In light of this, we proceeded to examine the levels of histamine and IL-31 (Fig. 6D and E). The results showed that treatment with osthole significantly decreased histamine and IL-31 levels in a dose-dependent manner. The highest osthole concentration showed the greatest reduction in histamine levels, while the moderate concentration had the most significant impact on IL-31 levels. To summarize, our findings indicated that osthole effectively reduced the level of inflammatory mediators.

3.5. Osthole inhibited expression of mRNA and protein of IL-31 and IL-31 RA in vitro

HaCaT cells were seeded at 5×10^4 cells per well of 96-well plates overnight and then treated with various concentrations of osthole (0.1, 0.3, 1, 3, 10, 30 μmol/L) for 24 h in a 37 °C incubator. The concentration of osthole less than 3 μmol/L did not alter cell viability in HaCaT cells (Fig. 7A and B). Therefore, concentrations of 0.3, 1 and 3 μmol/L osthole were selected for the subsequently cellular experiments in this study. The results showed that in the model group, both mRNA and protein expression levels of IL-31 RA were elevated, but they were significantly reduced following osthole treatment (Fig. 7D, E, and F). A similar trend was observed in the mRNA expression levels of IL-31 (Fig. 7C). In addition, immunofluorescence staining revealed that the IL-31 RA signal was weak in the cells of the control group. In the model group cells, IL-31 RA was primarily distributed in the cell membrane and cytoplasm. After treatment with osthole, both the fluorescence intensity and the intracellular distribution of IL-31 RA changed, especially in the group treated with 3 μmol/L osthole, where a significant reduction in the fluorescence signal was observed (Fig. 7G). These observations under the fluorescence microscope are consistent with the quantitative data from WB and qRT-PCR, further supporting the effectiveness of osthole in inhibiting the expression of IL-31 RA.

3.6. Osthole inhibited activation of NF-κB signaling pathway and promoted activation of PPARα and PPARγ in vitro

PPARα (Jung et al., 2017) and PPARγ (Karuppagounder et al., 2015) directly regulate AD, while NF-κB significantly influences its progression. The activation of NF-κB is inhibited by PPARγ within the context of the PPARγ/NF-κB signaling pathway, primarily targeting inflammation regulation (Yao, Gu, Jiang, & Che, 2022). In order to understand whether the NF-κB signaling pathway or PPAR is associated with the alleviative effect of osthole on AD,

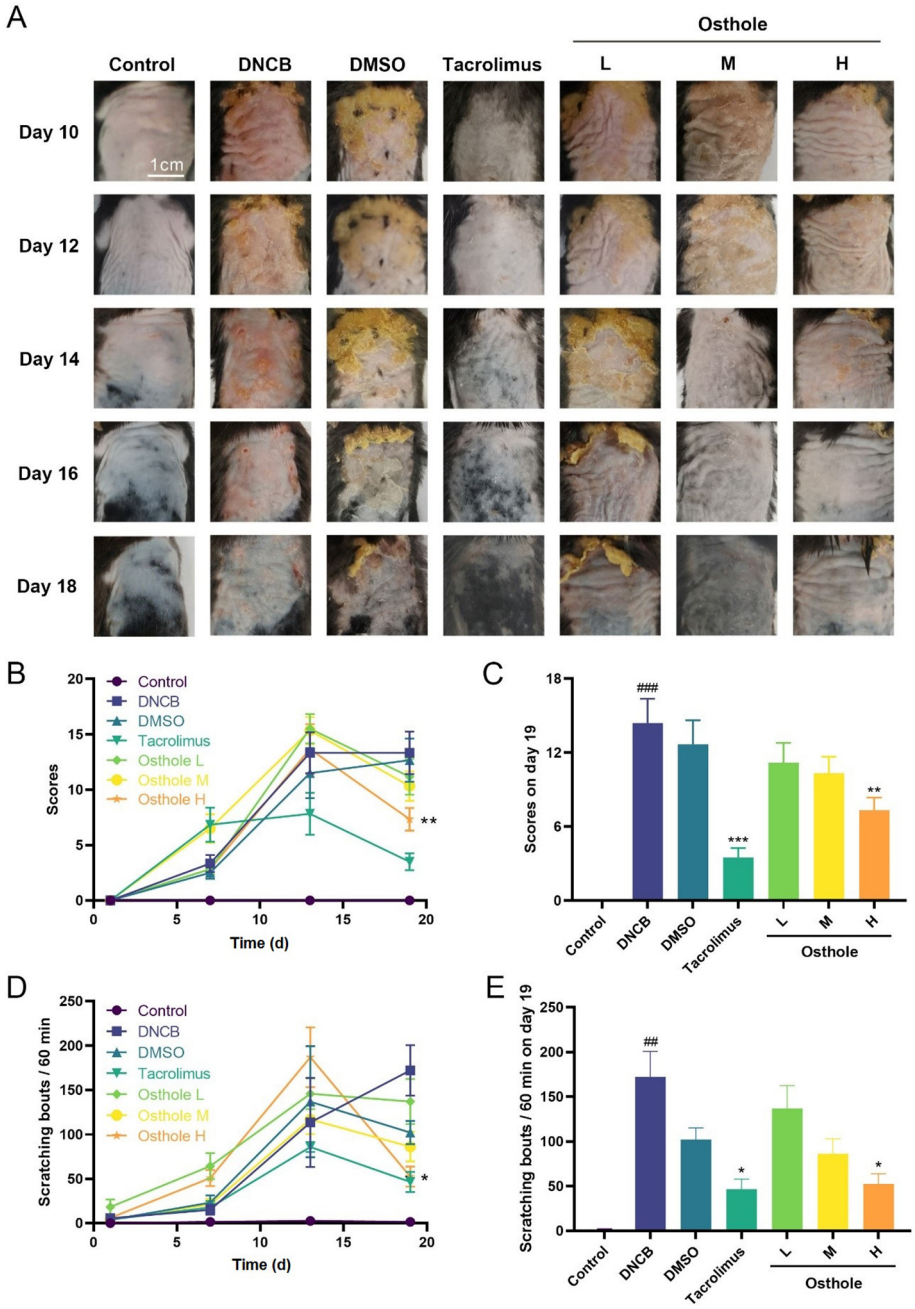

Fig. 2. Effect of osthole on DNCB-induced clinical features in mice. (A) Photographs of AD-like skin lesions of a representative mouse from each group. Scale bar: 1 cm. (B) Dermatitis score was quantified based on erythema, edema, erosion, dry skin and desquamation, and measured once a week for three weeks. (C) Score on day 19. (D) Number of scratching bouts in 60 min on day 1, 7, 13 and 19. (E) Scratching bouts in 60 min on day 19. Data are expressed as mean ± SEM, $n = 6$. ($^{\#\#}P < 0.01$, $^{\#\#\#}P < 0.001$ *vs* control group; $^{*}P < 0.05$, $^{**}P < 0.01$, $^{***}P < 0.001$ *vs* DNCB group. DMSO: DNCB + DMSO; L: osthole 5 mg/kg; M: osthole 25 mg/kg; H: osthole 50 mg/kg.).

we detected the expression of the protein IκBα, the phosphorylation of inhibitor of nuclear factor kappa-Bα (p-IκBα), p65, the phosphorylation of p65 (p-p65), and PPARα/γ. In HaCaT cells, IκBα increased significantly ($P < 0.01$), while the expressions of p-IκBα and p-p65 decreased ($P < 0.05$ and $P < 0.001$, respectively) in the osthole treatment group (3 μmol/L) (Fig. 8A–F). These changes suggested that osthole may regulate the levels of these proteins, possibly affecting inflammatory signaling pathways. On the other hand, PPARα and PPARγ were markedly ($P < 0.05$, $P < 0.01$, $P < 0.001$) promoted in all the osthole treatment groups (Fig. 8G–I). These results indicated that the remission of AD was related to the suppression of NF-κB and the activation of PPARα/γ.

3.7. PPAR involved in inhibited effect of osthole on IL-31 RA in vitro

To exam the role of PPAR in the effect of osthole on IL-31 RA, HaCaT cells were treated with osthole (1 μmol/L), osthole (1 μmol/L) + MK886 (an antagonist of PPARα), or osthole (1 μmol/L) + GW9662 (an antagonist of PPARγ). In the group treated solely with osthole, there was a decrease in both mRNA and protein expression of IL-31 RA. However, when MK886 and GW9662 were introduced, there was an increase in the mRNA and protein expression levels compared to the osthole-treated group alone (Fig. 9). These results confirmed that osthole improved the symptoms of AD by inhibiting the expression of IL-31 RA through activating PPARα and PPARγ.

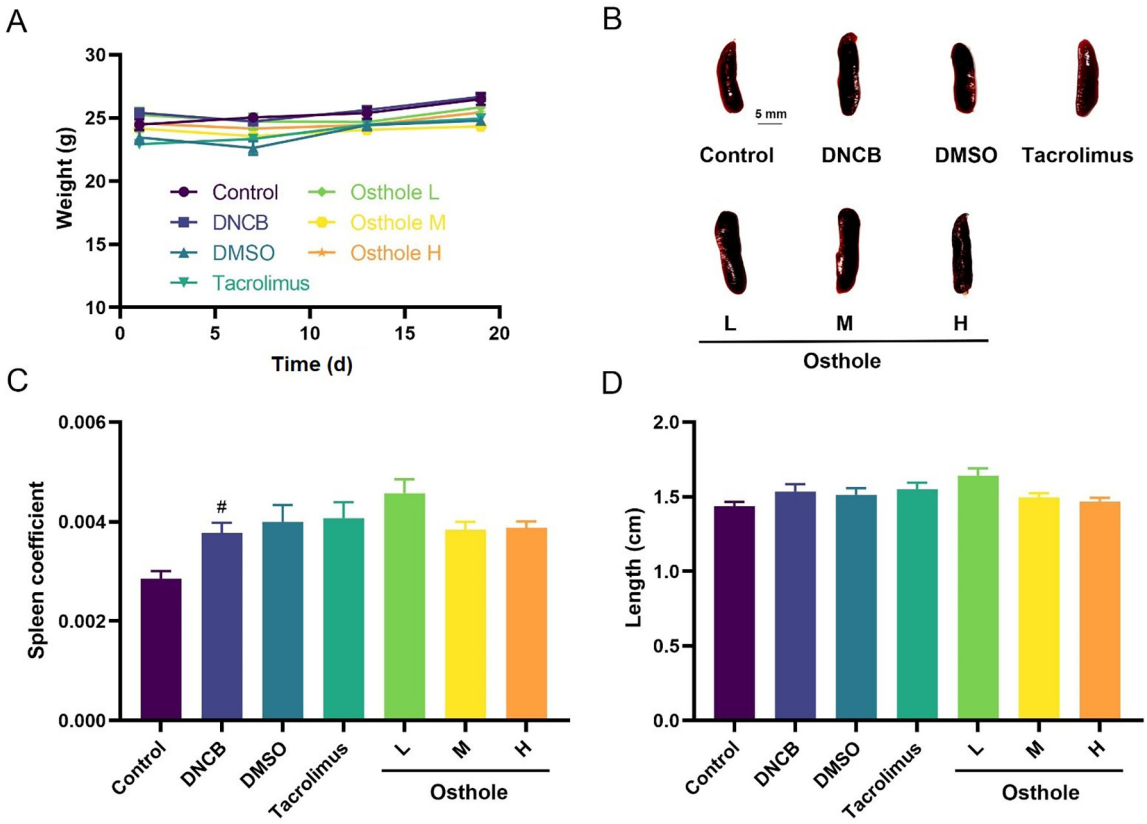

Fig. 3. Effect of osthole on spleen of DNCB-induced mice. (A) Weight changes of mice. (B) A representative spleen of mice in each group on day 21. Scale bar = 5 mm. (C) Spleen coefficient (Spleen to body weight ratio). (D) Length of spleen. Data are expressed as mean ± SEM, $n = 6$. ($^{\#}P < 0.05$ *vs* control group. DMSO: DNCB + DMSO; L: osthole 5 mg/kg; M: osthole 25 mg/kg; H: osthole 50 mg/kg.).

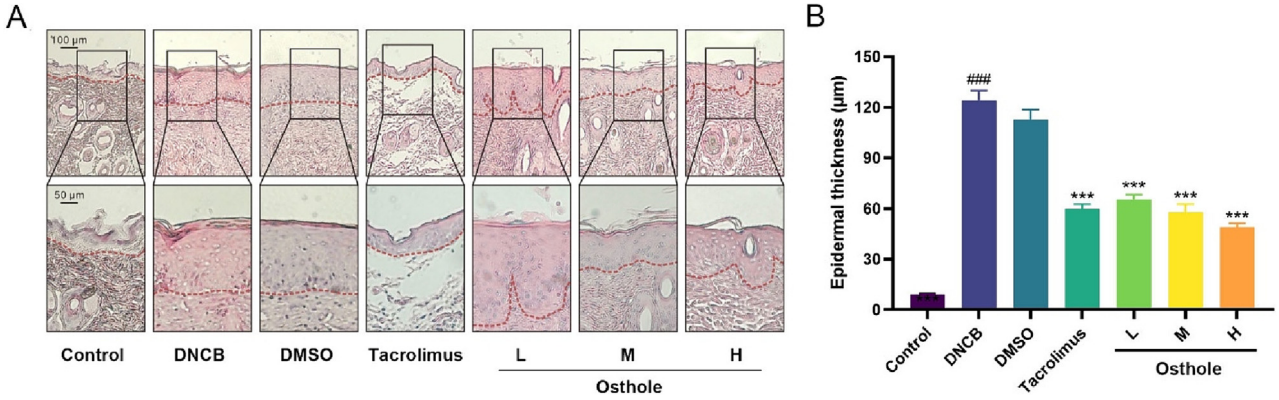

Fig. 4. Effect of osthole on DNCB-induced AD-like skin lesions. (A) Histopathological presentation of skin by H&E staining. Scale bar: 100 μm (magnification, × 100) or 50 μm (magnification, × 200). (B) Epidermal thickness in representative fields. Data are expressed as mean ± SEM, $n = 6$. ($^{\#\#\#}P < 0.001$ *vs* control group; $^{***}P < 0.001$ *vs* DNCB group. DMSO: DNCB + DMSO; L: osthole 5 mg/kg; M: osthole 25 mg/kg; H: osthole 50 mg/kg.).

4. Discussion

C. monnieri, renowned for its broad spectrum of pharmacological properties including anti-inflammatory, anti-allergic, and antiviral effects, has been effectively utilized in clinical practice for the treatment of various dermatoses (Wang, 2020), including genital eczema and scabies, as well as gynecopathy (Sun, Xie, Zhu, Xue, & Gu, 2009). Coumarin derivatives from *C. monnieri*, including imperatorin and xanthotoxol, exhibit potential in alleviating symptoms similar to those associated with AD. For instance, imperatorin has been shown to effectively alleviate symptoms related to psoriasis, including skin desquamation, epidermal thickening, keratinocyte hyperproliferation, and neutrophil infiltration (Tsai et al., 2021). Xanthotoxol administration, both intraperitoneally and intrathecally, has been shown to significantly reduce scratching behavior in mice induced by compound 48/80 or chloroquine. The effectiveness of xanthotoxol in alleviating symptoms of chronic pruritus has been observed in mice models with dry skin and allergic contact dermatitis (Gao et al., 2023).

Among the coumarins derived from *C. monnieri*, osthole is particularly distinguished for its remarkable abundance (Wu et al., 2020) and a wide range of salutary effects, which include

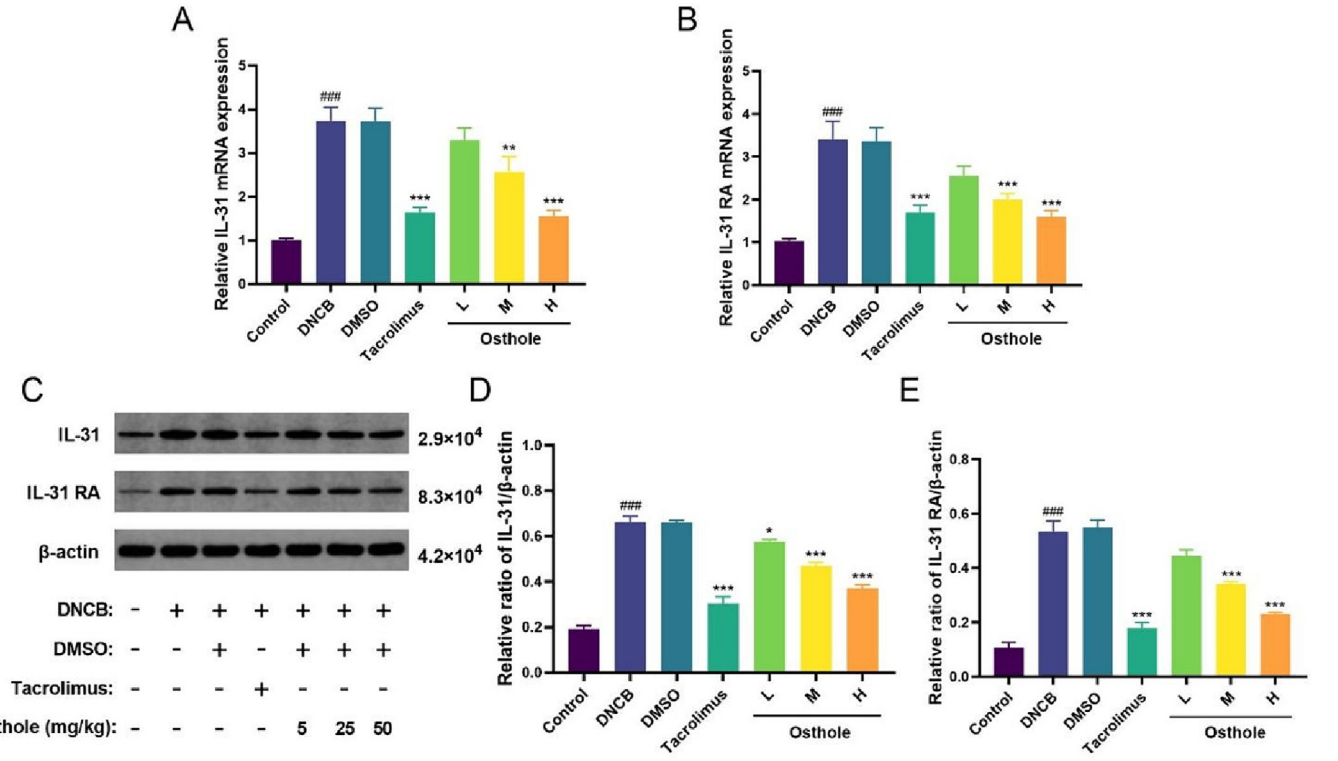

Fig. 5. Effect of osthole on IL-31 and IL-31 RA in skin of DNCB-induced mice. Relative mRNA expression of IL-31 (A) and IL-31 RA (B) in each group. (C) Protein expression levels of IL-31 and IL-31 RA in skin lesion of DNCB-induced mice detected by WB analysis. Quantified protein levels of IL-31 (D) and IL-31 RA (E) using gray value analyses by Image J software. Data are expressed as mean ± SEM, $n = 3$. ($^{\#\#\#}P < 0.001$ *vs* control group; $^{*}P < 0.05$, $^{**}P < 0.01$, $^{***}P < 0.001$ *vs* DNCB group. DMSO: DNCB + DMSO; L: osthole 5 mg/kg; M: osthole 25 mg/kg; H: osthole 50 mg/kg.).

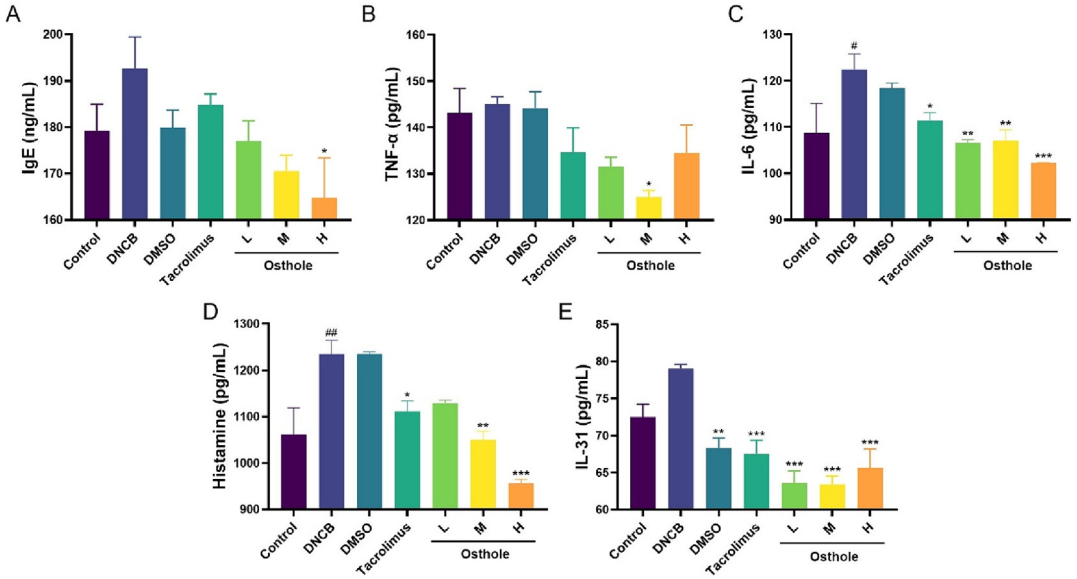

Fig. 6. Effect of osthole on serum inflammatory mediator in DNCB-induced C57BL/6J mice. (A-E) Total IgE, TNF-α, IL-6, histamine and IL-31 levels in serum detected using ELISA. Data are expressed as mean ± SEM, $n = 3$. ($^{\#}P < 0.05$, $^{\#\#}P < 0.01$ *vs* control group; $^{*}P < 0.05$, $^{**}P < 0.01$, $^{***}P < 0.001$ *vs* DNCB group. DMSO: DNCB + DMSO; L: osthole 5 mg/kg; M: osthole 25 mg/kg; H: osthole 50 mg/kg.).

anti-inflammatory, anti-oxidative (Zhang, Xie, Xue, & Gu, 2008), anti-histaminic (Hu et al., 2023), and immune-enhancing properties (Kordulewska et al., 2021), thereby it holds great potential for further research in the realm of skin diseases. At present, several studies have explored osthole analogues. Huang et al. designed and synthesized 23 compounds based on osthole. They observed that the structural composition of stilbene significantly influenced osthole's activity, and the introduction of indole acetic acid improved its activity (Huang et al., 2022). Another researcher, Li Zhang, from the same team, found that introducing piperazine-substituted carbamate and aromatic amine with tetrahydropyrrole into osthole enhanced its cytoprotective properties against H_2O_2

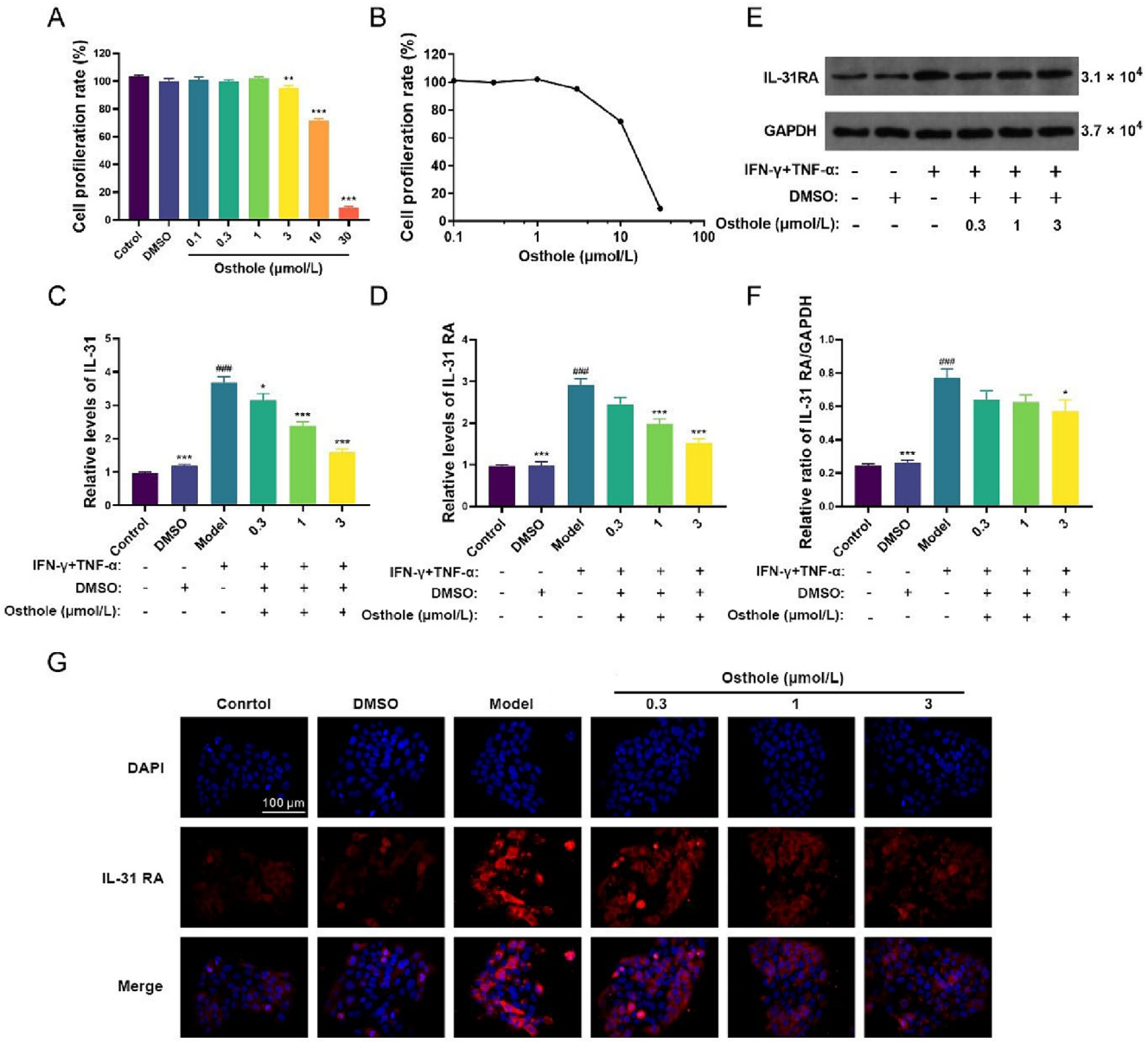

Fig. 7. Effect of osthole on expression of IL-31 and IL-31 RA in HaCaT cells. HaCaT cells was treated with osthole at different concentrations (0.1−30 μmol/L) for 24 h (A). Cell viability was measured by MTT assay (B). Relative levels of IL-31 (C) and IL-31 RA (D) gene expression determined by RT-qPCR. (E and F) Protein expressions of IL-31 RA *in vitro* determined by WB. (G) HaCaT cells were pretreated with 0.3, 1, or 3 μmol/L osthole for 1 h and further incubated with 10 ng/mL IFN-γ/TNF-α for 1 h. Cells showed blue fluorescence after DAPI staining, and IL-31 RA showed red fluorescence was stained with a CY3 Conjugated AffiniPure rabbit anti-goat IgG antibody. (scale bar = 100 μm, magnification, × 200). Data are expressed as mean ± SEM, n = 3. ($^{\#\#\#}P < 0.001$ *vs* control group; $^{*}P < 0.05$, $^{***}P < 0.001$ *vs* model group. DMSO: DMSO only.).

and OGD. Furthermore, adding an aromatic amine with a tetrahydropyrrole structure increased osthole's NO inhibitory abilities (Zhang et al., 2020). The speculative potential of osthole and its analogues for AD treatment research lies in their influence on mast cell functionality and the comprehensive pharmacological actions of osthole (McCauley, Gilchrist, & Befus, 2005), including anti-inflammatory and anti-oxidative effects. These actions collectively contribute to mitigating AD symptoms. Therefore, we speculate that osthole analogues may offer benefits for AD treatment research.

The primary pathogenesis of AD is immune dysfunction, which is characterized by the up-regulation of IgE levels, T cell expression, and immune cytokines in keratinocytes, dendritic cells, and mast cells. Consequently, the treatment of AD should focus on inhibiting the expression of inflammatory factors and blocking the inflammatory signaling pathway. AD-like cutaneous lesions are characterized by epidermal hyperplasia and hyperkeratosis (Kim et al., 2023). Previous research indicates that osthole has the ability to enhance the skin barrier (Qin et al., 2018) and alleviate inflammation (Ashrafizadeh et al., 2020) in individuals suffering from AD, suggesting potential clinical applications. In this study, the administration of DNCB to the mice's dorsal region resulted in visible signs of white scales, erythema, and ulceration on the dermal surface, accompanied by an increased skin injury score and elevated scratching behavior. Histological examination using H&E staining revealed pathological features such as hyperkeratosis and epidermal hypertrophy, confirming the successful establishment of an AD model. The subsequent administration of osthole via gavage notably alleviated AD-like symptoms in mice, indicated by reduced epidermal thickness and improved skin condition. For instance, Fu et al.'s study supported the therapeutic efficacy of osthole for AD in mice, showing a significant decrease in

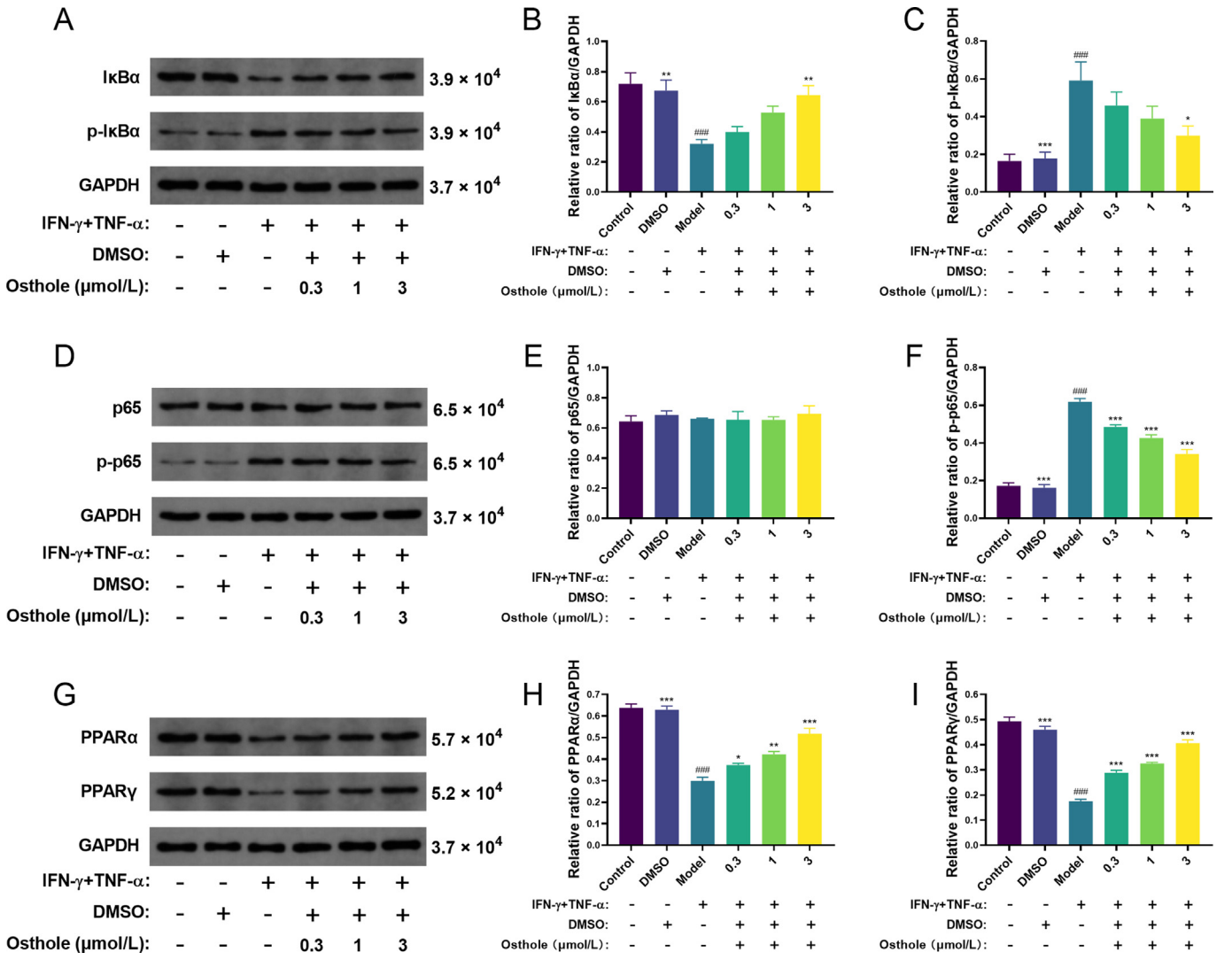

Fig. 8. Osthole suppressed IκBα, p65 phosphorylation and upregulated protein expression of PPARα and PPARγ *in vitro*. WB of IκBα (A–C) or p65 phosphorylation (D–F), PPARα and PPARγ in HaCaT cells (G–I). Protein levels were quantified using gray value analyses by Image J software. Data are mean ± SEM, $n = 3$. ($^{###}P < 0.001$ *vs* control group; $^{*}P < 0.05$, $^{**}P < 0.01$, $^{***}P < 0.001$ *vs* model group. DMSO: DMSO only.).

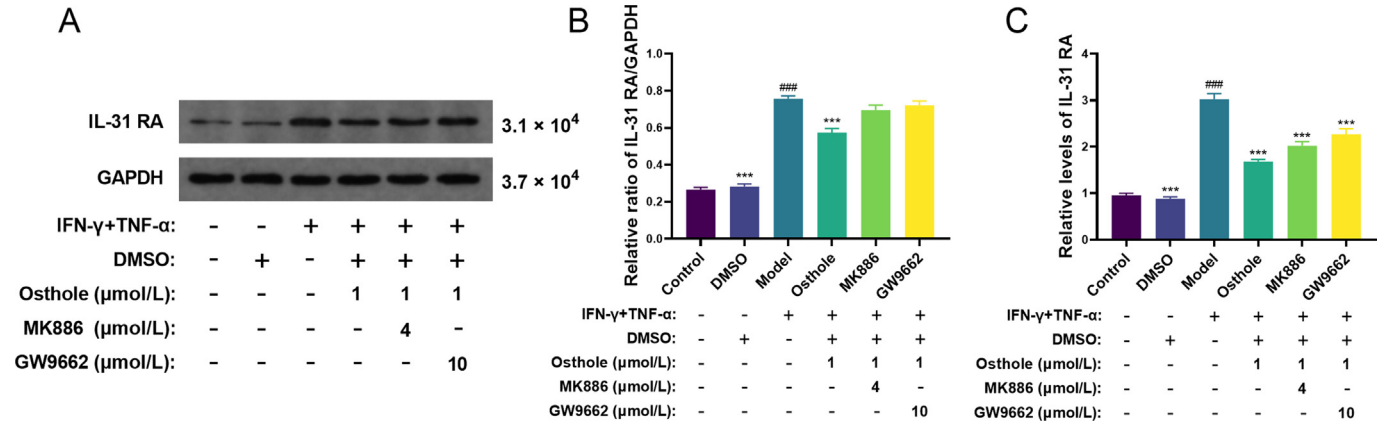

Fig. 9. Effect of antagonist of PPARα (MK886) and PPARγ (GW9662) on expression of IL-31 RA in HaCaT cells. Protein expressions of IL-31 RA in HaCaT cells were determined by WB(A and B). Relative levels of IL-31 RA gene expression *in vitro* were determined by qPCR (C). Data are expressed as mean ± SEM, $n = 3$. ($^{###}P < 0.001$ *vs* control group; $^{***}P < 0.001$ *vs* model group. DMSO: DMSO only.).

epidermal thickness (Fu & Hong, 2019). However, the study did not observe the effect on skin damage or consider the antipruritic properties of osthole. For a deeper understanding of osthole's anti-inflammatory and antipruritic qualities, we investigated inflammatory markers in mouse serum. TNF-α, a cytokine primarily secreted by keratinocytes (Asahina & Maeda, 2017), inhibits cell proliferation, promotes IL-6 expression, and contributes to the generation of macrophage-derived chemokines (MDCs) and thymus activation regulated chemokine (TARCs) via the NF-κB signaling pathway (Oh et al., 2022). IL-6 significantly impacts the pathogenesis of autoimmune disorders and chronic inflammatory conditions. Moreover, patients with AD exhibit elevated levels of IL-6 in their keratinocytes (Huang et al., 2023). The results of our testing indicated that the administration of osthole led to a significant decrease in the levels of IgE, TNF-α, histamine, and IL-6 in the serum of mice, which demonstrated that osthole possessed the capacity to ameliorate symptoms of AD by suppressing the production of various inflammatory mediators. Thus, osthole has potential as a viable treatment option for AD in a clinical setting.

Chronicity, the defining feature of AD, involves inflammation, IgE-mediated allergen sensitization, epidermal barrier damage, and CP. CP, persisting for over six weeks, constitutes one of the most distressing symptoms for AD patients, often leading to sleep disturbances and reduced quality of life (Tang & Yao, 2022). The intricate mechanism behind CP development intertwines various factors such as neural pathways, immune regulation, skin barrier function, activity of itch mediators and receptors, and external environmental influences (Hu, 2021).

IL-31 is a member of the gp130/IL-6 cytokine family, and its primary source of production is Th2 cells. The expression of IL-31 can be induced by activating STAT6 and transmitting signals through IL-4, and activating NF-κB via IL-33 (Furue & Furue, 2021). IL-31 is the principal cytokine responsible for inducing itching in AD, and it is found to be upregulated in the epithelial cells of affected individuals and mouse models (Kim et al., 2023). In this study, we conducted tests on the dorsal skin of mice and observed that those in the model group, which exhibited more severe itching behavior, had higher levels of IL-31 in the serum of the mice, and expression levels of IL-31, IL-31 RA on their skin. Conversely, treatment with varying concentrations of osthole resulted in a dose-dependent decrease in the expression levels of IL-31 and IL-31 RA on the skin of mice, leading to a reduction in itching behavior.

NF-κB is a cytoplasmic transcription factor that plays a crucial role in immune and inflammatory responses (Kim et al., 2021b). The NF-κB consists of a dimer of p50 and p65 proteins and is usually associated with IκB in an inactive form, forming a complex in the cytoplasm. This complex can be activated by various ligands, such as TNF-α, when stimulated by oxidative stress, pro-inflammatory factors, ultraviolet radiation, and other factors (Li et al., 2022). Upon activation, IκB undergoes phosphorylation and degradation, and the NF-κB p65/p50 dimer is translocated into the nucleus and binds to DNA in a phosphorylated form. This induces the expression of various proinflammatory cytokine genes, thereby activating the NF-κB signal in an autocrine manner (Kim et al., 2022). It is responsible for activating various cytokines and mediators related to immune and inflammation, which are essential in the pathogenesis of AD (Fan et al., 2018). Prior research has demonstrated that the advancement of AD is heavily influenced by the involvement of NF-κB (Kim et al., 2021b). Additionally, it has been found that NF-κB can serve as a mediator for the expression of IL-31 induced by IL-4/IL-33 (Maier, Werner, Duschl, Bohle, & Horejs-Hoeck, 2014). For a more comprehensive understanding of osthole's anti-inflammatory properties, we conducted an investigation to evaluate its impact on the NF-κB signaling pathway. Earlier investigations have indicated that the involvement of NF-κB in IL-6, IL-8, and IL-1β is pivotal in the creation of pro-inflammatory agents (Oh et al., 2022). Conversely, impeding the activation of the NF-κB signaling pathway can curtail the expression of various inflammatory factors and ameliorate the inflammatory response (Fan et al., 2018). For instance, a study discovered that fisetin had a dual effect on AD mice by not only reducing their scratching behavior, but also by impeding the phosphorylation process of NF-κB and delaying the development of IκBα, which ultimately hindered the nuclear translocation of NF-κB (Che et al., 2018). Hong et al. conducted a study wherein they employed solanum nigrum to intervene in an inflammation model induced by TNF-α and IFN-γ in HaCaT. The findings revealed a noteworthy reduction in the expression of p-NF-κB protein, and a down-regulation of NF-κB mRNA levels (Hong et al., 2020). Following the investigation of the principal protein of the NF-κB signaling pathway, we discovered that osthole can hinder the phosphorylation of IκBα in conjunction with p65 in a dose-dependent manner. This suggests that osthole can effectively impede the activation of the NF-κB signaling pathway, thereby mitigating inflammation associated with AD.

As a transcription factor activated by ligands, PPAR has the ability to impede the expression of inflammatory factors and the progression of inflammation (Stark, Coquet, & Tibbitt, 2021). The utilization of PPARα agonists resulted in diminished skin inflammation, reduced epidermal thickening, decreased infiltration of inflammatory cells in the dermis, and an amelioration of AD (Jung et al., 2017). PPARγ, a vital transcription factor that regulates lipid metabolism, exhibits high expression in immune cells and tissues, playing a potential role in immune regulation by promoting the differentiation and maturation of dendritic cells. Yao et al. has utilized PPARγ as a potential therapeutic target for inflammatory and allergic diseases. Moreover, ovalbumin induced allergic model mice were treated with rosiglitazone, a PPARγ agonist, which resulted in the inhibition of p65 protein expression and a decrease in PAK1 and pPAK1 levels (Yao et al., 2022). Based on these findings, the researchers have proposed the PPARγ-NF-κB-pPAK1 cascade reaction as a promising target for the treatment of such conditions. The regulation of inflammation is a key target of the PPARγ/NF-κB signal pathway, and the activation of PPARγ can be indirectly modulated by the activity of NF-κB, leading to the inhibition of inflammatory reactions (Wang, Sun, & Liu, 2021). Research has indicated that the absence of the PPAR gene in mice results in a marked elevation of inflammatory factors such as IL-1, IL-6, and TNF-α, leading to a corresponding increase in tissue inflammation (Li et al., 2022). The activation of PPARα by eupatilin has the potential to impact the phosphorylation process of IκB, leading to the inhibition of TNF-α induced NF-κB activation. Eupatilin regulates the expression of MMP-2/-9 and inhibits the nuclear translocation of NF-κB, thereby alleviating inflammatory reactions (Jung et al., 2017). Moreover, PPARα and PPARγ play a direct role in the regulation of AD (He, Qiu, Chen, Li, & Wu, 2022). For instance, pioglitazone triggers PPARγ receptors to suppress itching (Ostadhadi, Nikoui, Haj-Mirzaian, Kordjazy, & Dehpour, 2015). PPARα agonists have been shown to reduce dermal inflammatory cell infiltration in AD mice induced by house dust mites, slow down the increase of serum IgE, and inhibit the expression of various inflammatory factors such as IL-4, IL-1β, IFN-γ, and TNF-α (Karuppagounder et al., 2015). To assess the impact of osthole on AD through PPARα and PPARγ, we conducted an experiment with TNF-α and IFN-γ as inducing agents on HaCaT cells to create an inflammatory model similar to that of AD (Lee et al., 2020). In regards to human AD, it has been established that keratinocytes secrete various soluble elements, which can stimulate Th2-associated inflammation when those exposed to allergens or bacteria (Asahina & Maeda, 2017). The activation of keratinocytes is initiated by a variety of cytokines released by immune cells. Once activated, these keratinocytes produce

pro-inflammatory cytokines, including IL-6 and TNF-α, which serve to intensify inflammatory lesions through both autocrine and paracrine mechanisms (Choi et al., 2019). The inhibitory effect of osthole on the expression levels of IL-31 RA under stimulation has been confirmed, along with its impact on TNF-α and IFN-γ. This effect can be reversed by MK886 and GW9662. Furthermore, osthole can serve as a stimulant for PPARα and PPARγ, leading to their upregulation. These findings suggest that osthole can effectively alleviate inflammatory responses by inhibiting the expression of IL-31 RA through PPARα and PPARγ activation.

To summarize, our investigation delved into the effects of osthole on CP in AD and its underlying mode of operation. The expression of IL-31 is downregulated by osthole through the activation of PPARα and PPARγ, as well as the inhibition of the NF-κB signaling pathway. The current study is restricted in the exploration of PPAR, which is restricted to the cellular level, and there has been no examination conducted for PPARβ. In future research, we will investigate the impact of osthole on the expression of three PPAR subtypes in animals.

5. Conclusion

This study aimed to investigate the anti-inflammatory and antipruritus effects and mechanisms of osthole on DNCB-induced AD. Following the application of DNCB to induce AD-like skin lesions in C57BL/6J mice and subsequent treatment with osthole, we observed an improvement in skin damage, a decrease in epidermal thickness, a reduction in scratching behavior, and an inhibition of inflammatory reactions. The activation of PPARα and PPARγ generation by osthole, along with the inhibition of NF-κB, has been observed to downregulate exprssion of IL-31 and IL-31 RA. This process has been found to reduce skin damage and CP associated with AD, making osthole a potential drug for clinical treatment of AD.

CRediT authorship contribution statement

Shuang He: Validation, Methodology, Data curation, Formal analysis, Writing – original draft, Writing – review & editing, Funding acquisition. **Xiaoling Liang:** Formal analysis, Writing – original draft. **Weixiong Chen:** Methodology, Data curation, Formal analysis. **Yangji Nima:** Data curation. **Yi Li:** Data curation. **Zihui Gu:** Methodology. **Siyue Lai:** Methodology. **Fei Zhong:** Methodology. **Caixiong Qiu:** Methodology. **Yuying Mo:** Data curation. **Jiajun Tang:** Data curation. **Guanyi Wu:** Conceptualization, Validation, Methodology, Formal analysis, Resources, Writing – review & editing, Funding acquisition.

Declaration of Competing Interest

The authors declare that they have no known competing financial interests or personal relationships that could have appeared to influence the work reported in this paper.

Acknowledgments

This work was supported by the Natural Science Foundation of China (NSFC) to Guanyi Wu (No. 82060768); the Natural Science Foundation of Guangxi Zhuang Autonomous Region (No. 2020GXNSFAA297244); Innovation Project of Guangxi Graduate Education (No. YCSW2023392); an Open Project of the Guangxi University of Chinese Medicine Top Disciplines Construction Project (No. 2018XK022); an Open Project of the Guangxi Key Laboratory of Zhuang and Yao Ethnic Medicine (No. GXZYKF2020-07); Guipai Traditional Chinese Medicine Top-Notch Talent Funding Project from Guangxi University of Chinese Medicine (No. 2022C001); the Second and Third Batch of the "Qihuang Project" High-Level Talent Team Cultivation Project of Guangxi University of Traditional Chinese Medicine (No. 2021001 and No. 202402).

References

Asahina, R., & Maeda, S. (2017). A review of the roles of keratinocyte-derived cytokines and chemokines in the pathogenesis of atopic dermatitis in humans and dogs. *Veterinary Dermatology, 28*(1), 16–e5.

Ashrafizadeh, M., Mohammadinejad, R., Samarghandian, S., Yaribeygi, H., Johnston, T. P., & Sahebkar, A. (2020). Anti-tumor effects of osthole on different malignant tissues: A review of molecular mechanisms. *Anti-Cancer Agents in Medicinal Chemistry, 20*(8), 918–931.

Barequet, I. S., Platner, E., Sade, K., Etkin, S., Ziv, H., Rosner, M., & Habot-Wilner, Z. (2013). Topical tacrolimus for the management of acute allergic conjunctivitis in a mouse model. *Graefe's Archive for Clinical and Experimental Ophthalmology, 251*(7), 1717–1721.

Cevikbas, F., Wang, X., Akiyama, T., Kempkes, C., Savinko, T., Antal, A., ... Steinhoff, M. (2014). A sensory neuron–expressed IL-31 receptor mediates T helper cell–dependent itch: Involvement of TRPV1 and TRPA1. *Journal of Allergy and Clinical Immunology, 133*(2), 448–460.

Che, D. N., Cho, B. O., Shin, J. Y., Kang, H. J., Kim, Y. S., & Jang, S. I. (2018). Fisetin inhibits IL-31 production in stimulated human mast cells: Possibilities of fisetin being exploited to treat histamine-independent pruritus. *Life Sciences, 201*, 121–129.

Chen, X., Zhu, C., Zhang, Y., Yang, N., Shi, H., Yang, W., ... Tang, Z. (2020). Antipruritic effect of ethyl acetate extract from fructus cnidii in mice with 2,4-dinitrofluorobenzene-induced atopic dermatitis. *Evidence-Based Complementary and Alternative Medicine, 2020*, 1–14.

Choi, Y. A., Yu, J. H., Jung, H. D., Lee, S., Park, P. H., Lee, H. S., ... Kim, S. H. (2019). Inhibitory effect of ethanol extract of Ampelopsis brevipedunculata rhizomes on atopic dermatitis-like skin inflammation. *Journal of Ethnopharmacology, 238*, 111850.

Cornelissen, C., Marquardt, Y., Czaja, K., Wenzel, J., Frank, J., Lüscher-Firzlaff, J., ... Baron, J. M. (2012). IL-31 regulates differentiation and filaggrin expression in human organotypic skin models. *Journal of Allergy and Clinical Immunology, 129*(2), 426–433.

Dou, X., Zhong, W., Wu, X., Chen, S., Shao, Y., & Zhang, J. (2018). Expression of interleukin 31 and its receptors in prurigo nodularis. *The Chinese Journal of Dermatovenereology, 32*(10), 1134–1138.

Duca, E., Sur, G., Armat, I., Samasca, G., & Sur, L. (2022). Correlation between Interleukin 31 and clinical manifestations in children with atopic dermatitis: An observational study. *Allergologia et Immunopathologia, 50*(1), 75–79.

Fan, H. J., Xie, Z. P., Lu, Z. W., Tan, Z. B., Bi, Y. M., Xie, L. P., ... Zhou, Y. C. (2018). Anti-inflammatory and immune response regulation of Si-Ni-San in 2,4-dinitrochlorobenzene-induced atopic dermatitis-like skin dysfunction. *Journal of Ethnopharmacology, 222*, 1–10.

Frazier, W., & Bhardwaj, N. (2020). Atopic dermatitis: Diagnosis and treatment. *Atopic Dermatitis, 101*(10), 9.

Fu, X., & Hong, C. (2019). Osthole attenuates mouse atopic dermatitis by inhibiting thymic stromal lymphopoietin production from keratinocytes. *Experimental Dermatology, 28*(5), 561–567.

Furue, M., & Furue, M. (2021). Interleukin-31 and pruritic skin. *Journal of Clinical Medicine, 10*(9), 1906.

Gao, X., Yang, Y., Zhu, J., Zhang, Y., Wang, C., Wang, Z., ... Du, L. (2023). Xanthotoxol relieves itch in mice via suppressing spinal GRP/GRPR signaling. *European Journal of Pharmacology, 960*, 176147.

Guilloteau, K., Paris, I., Pedretti, N., Boniface, K., Juchaux, F., Huguier, V., ... Morel, F. (2010). Skin inflammation induced by the synergistic action of IL-17A, IL-22, oncostatin M, IL-1α, and TNF-α recapitulates some features of psoriasis. *The Journal of Immunology, 184*(9), 5263–5270.

He, S., Qiu, C., Chen, W., Li, K., & Wu, G. (2022). The role of peroxisome proliferator-activated receptor in atopic dermatitis. *The Chinese Journal of Dermatovenereology, 37*(10), 1–10.

Hong, S., Lee, B., Kim, J., Kim, E., Kim, M., Kwon, B., ... Jung, H. (2020). Solanum nigrum Linne improves DNCB-induced atopic dermatitis-like skin disease in BALB/c mice. *Molecular Medicine Reports, 22*(4), 2878–2886.

Hu, S. (2021). Advances in diagnosis and treatment of atopic dermatitis. *China Modern Medicine, 28*(28), 25–28.

Hu, X., Zhou, Y., Shi, J., Qi, M., Li, X., Yang, Y., ... Yu, G. (2023). Osthole relieves skin damage and inhibits chronic itch through modulation of Akt/ZO-3 pathway in atopic dermatitis. *European Journal of Pharmacology, 947*, 175649.

Huang, S., Wang, H., Zheng, H., Li, W., Shi, J., Shen, C., & Tao, R. (2023). Association between IL-6 polymorphisms and atopic dermatitis in Chinese Han children. *Frontiers in Pediatrics, 11*, 1156659.

Huang, W., Huang, Y., Cui, J., Wu, Y., Zhu, F., Huang, J., & Ma, L. (2022). Design and synthesis of Osthole-based compounds as potential Nrf2 agonists. *Bioorganic & Medicinal Chemistry Letters, 61*, 128547.

Jiang, W., & Wang, X. (2016). Progress of interleukin-4 in atopic dermatitis. *Journal of Clinical Dermatology, 45*(10), 742–745.

Jung, Y., Kim, J. C., Choi, Y., Lee, S., Kang, K. S., Kim, Y. K., & Kim, S. N. (2017). Eupatilin with PPARα agonistic effects inhibits TNFα-induced MMP signaling in HaCaT cells. *Biochemical and Biophysical Research Communications, 493*(1), 220–226.

Karuppagounder, V., Arumugam, S., Thandavarayan, R. A., Pitchaimani, V., Sreedhar, R., Afrin, R., ... Watanabe, K. (2015). Tannic acid modulates NFκB signaling pathway and skin inflammation in NC/Nga mice through PPARγ expression. *Cytokine, 76*(2), 206–213.

Kim, E. Y., Hong, S., Kim, J. H., Kim, M., Lee, Y., Sohn, Y., & Jung, H. S. (2021a). Effects of chloroform fraction of *Fritillariae Thunbergii Bulbus* on atopic symptoms in a DNCB-induced atopic dermatitis-like skin lesion model and *in vitro* models. *Journal of Ethnopharmacology, 281*, 114453.

Kim, H. J., Song, H. K., Park, S. H., Jang, S., Park, K. S., Song, K. H., ... Kim, T. (2022). *Terminalia chebula* Retz. extract ameliorates the symptoms of atopic dermatitis by regulating anti-inflammatory factors *in vivo* and suppressing STAT1/3 and NF-κB signaling *in vitro*. *Phytomedicine, 104*, 154318.

Kim, H. M., Kang, Y. M., Jin, B. R., Lee, H., Lee, D. S., Lee, M., & An, H. J. (2023). Morus alba fruits attenuates atopic dermatitis symptoms and pathology *in vivo* and *in vitro* via the regulation of barrier function, immune response and pruritus. *Phytomedicine, 109*, 154579.

Kim, J. H., & Kim, W. (2022). Alleviation effects of *Rubus coreanus* Miquel root extract on skin symptoms and inflammation in chronic atopic dermatitis. *Food & Function, 13*(5), 2823–2831.

Kim, S. Y., Han, S. D., Kim, M., Mony, T. J., Lee, E. S., Kim, K. M., ... Park, S. J. (2021b). *Mentha arvensis* essential oil exerts anti-inflammatory in LPS-stimulated inflammatory responses via inhibition of ERK/NF-κb signaling pathway and anti-atopic dermatitis-like effects in 2,4-dinitrochlorobezene-induced balb/c mice. *Antioxidants, 10*(12), 1941.

Kordulewska, N. K., Topa, J., Stryiński, R., & Jarmołowska, B. (2021). Osthole inhibits expression of genes associated with toll-like receptor 2 signaling pathway in an organotypic 3D skin model of human epidermis with atopic dermatitis. *Cells, 11*(1), 88.

Lee, J., Ki, H., Kim, D., & Lee, Y. (2018). Triticum aestivum sprout extract attenuates 2,4-dinitrochlorobenzene-induced atopic dermatitis-like skin lesions in mice and the expression of chemokines in human keratinocytes. *Molecular Medicine Reports, 18*(3), 3461–3468.

Lee, J. H., Lim, J. Y., Jo, E. H., Noh, H. M., Park, S., Park, M. C., & Kim, D. K. (2020). *Chijabyukpi-tang* inhibits pro-inflammatory cytokines and chemokines via the nrf2/ho-1 signaling pathway in TNF-α/IFN-γ-stimulated hacat cells and ameliorates 2,4-dinitrochlorobenzene-induced atopic dermatitis-like skin lesions in mice. *Frontiers in Pharmacology, 11*, 1018.

Li, B., Li, L., Xie, F., Guo, D., Zhang, H., Huang, X., ... Guan, W. (2022). Advances in the regulation of inflammatory signaling pathways by peroxisome proliferators-activated receptor-γ. *Chinese Journal of Animal Science, 58*(1), 32–37.

Li, K., Qiu, C., He, S., Huang, C., & Wu, G. (2022). Research progress of the correlations between interleukin-31 and pruritus. *Journal of Guangxi Normal University (Natural Science Edition), 41*(2), 1–12.

Li, N., Heng, M., & Wang, J. (2022). Discussion on new drugs and clinical pharmacology studies for atopic dermatitis. *Drug Evaluation Research, 45*(9), 1894–1902.

Maier, E., Werner, D., Duschl, A., Bohle, B., & Horejs-Hoeck, J. (2014). Human Th2 but not Th9 cells release IL-31 in a STAT6/NF-κB-dependent way. *Journal of Immunology, 193*(2), 645–654.

McCauley, S., Gilchrist, M., & Befus, A. (2005). Nitric oxide: A major determinant of mast cell phenotype and function. *Memórias Do Instituto Oswaldo Cruz, 100*(suppl 1), 11–14.

Meng, J., Li, Y., Fischer, M. J. M., Steinhoff, M., Chen, W., & Wang, J. (2021). Th2 modulation of transient receptor potential channels: An unmet therapeutic intervention for atopic dermatitis. *Frontiers in Immunology, 12*, 696784.

Meng, X., Liu, F., Wang, F., Yang, J., Wang, H., & Xie, G. (2018). Protective effects of osthole against inflammation induced by lipopolysaccharide in BV2 cells. *Molecular Medicine Reports, 17*(3), 4561–4566.

No, H., Nam, S. H., Seo, H. W., Seo, J., Park, S. H., Kim, S. B., ... Kim, J. K. (2021). Purple corn extract alleviates 2,4-dinitrochlorobenzene-induced atopic dermatitis-like phenotypes in BALB/c mice. *Animal Cells and Systems, 25*(5), 272–282.

Oh, J. H., Kim, S. H., Kwon, O. K., Kim, J. H., Oh, S. R., Han, S. B., ... Ahn, K. S. (2022). Purpurin suppresses atopic dermatitis via TNF-α/IFN-γ-induced inflammation in HaCaT cells. *International Journal of Immunopathology and Pharmacology, 36*, 3946320221111135.

Ostadhadi, S., Nikoui, V., Haj-Mirzaian, A., Kordjazy, N., & Dehpour, A. R. (2015). The role of PPAR-gamma receptor in pruritus. *European Journal of Pharmacology, 762*, 322–325.

Qin, X., Hu, Z., Zhang, H., & Mao, H. (2018). Study on the pharmacological effects and related mechanisms of osthole. *Tianjin Journal of Traditional Chinese Medicine, 35*(11), 877–880.

Sadraei, H., Shokoohinia, Y., Sajjadi, S. E., & Ghadirian, B. (2012). Antispasmodic effect of osthole and *Prangos ferulacea* extract on rat uterus smooth muscle motility. *Research in Pharmaceutical Sciences, 7*(3), 141.

Silverberg, J. I., Gelfand, J. M., Margolis, D. J., Boguniewicz, M., Fonacier, L., Grayson, M. H., ... Chiesa Fuxench, Z. C. (2018). Patient burden and quality of life in atopic dermatitis in US adults. *Annals of Allergy, Asthma & Immunology, 121*(3), 340–347.

Song, H. K., Park, S. H., Kim, H. J., Jang, S., & Kim, T. (2022). *Spatholobus suberectus* Dunn water extract ameliorates atopic dermatitis–like symptoms by suppressing proinflammatory chemokine production *in vivo* and *in vitro*. *Frontiers in Pharmacology, 13*, 14.

Stark, J. M., Coquet, J. M., & Tibbitt, C. A. (2021). The role of PPAR-γ in allergic disease. *Current Allergy and Asthma Reports, 21*(11), 45.

Sun, F., Xie, M. L., Zhu, L. J., Xue, J., & Gu, Z. L. (2009). Inhibitory effect of osthole on alcohol-induced fatty liver in mice. *Digestive and Liver Disease, 41*(2), 127–133.

Tang, Y., & Yao, Z. (2022). Research and therapy progress on the mechanisms of pruritus in atopic dermatitis. *Medical Journal of Peking Union Medical College Hospital, 13*(3), 473–479.

Tsai, Y. F., Chen, C. Y., Lin, I. W., Leu, Y. L., Yang, S. C., Syu, Y. T., ... Hwang, T. L. (2021). Imperatorin alleviates psoriasiform dermatitis by blocking neutrophil respiratory burst, adhesion, and chemotaxis through selective phosphodiesterase 4 inhibition. *Antioxidants & Redox Signaling, 35*(11), 885–903.

Wang, J. (2020). Interpretation of Chinese guidelines for the diagnosis and treatment of atopic dermatitis (2020). *Diagnosis and Therapy Journal of Dermato-Venereology, 27*(5), 359–361.

Wang, R., Sun, Z., & Liu, J. (2021). Catalpol alleviates liver injury in T2DM rats through PPARγ/NF-κB signaling pathway. *Chinese Journal of Pathophysiology, 37*(12), 2189–2196.

Wu, B., Sheng, X., Xu, Z., Zhang, Y., Dan, Y., Guo, J., ... Li, G. (2020). Osthole relieves diabetics cardiac autonomic neuropathy associated with P2X3 receptor in ratstellate ganglia. *Brain Research Bulletin, 157*, 90–99.

Xia, T., Li, L., & Chen, H. (2022). Research progress of itch related ion channels. *Acta Medicinae Universitatis Scientiae et Technologiae Huazhong (Medical Science), 51*(1), 114–119.

Yang, C. C., Hung, Y. L., Ko, W. C., Tsai, Y. J., Chang, J. F., Liang, C. W., ... Hung, C. F. (2021a). Effect of neferine on DNCB-induced atopic dermatitis in HaCaT cells and BALB/c mice. *International Journal of Molecular Sciences, 22*(15), 8237.

Yang, N., Ju, Y., Huang, D., Ling, K., Jin, H., Liu, J., ... Wu, G. (2021b). Desensitization of TRPV1 involved in the antipruritic effect of osthole on histamine-induced scratching behavior in mice. *Evidence-Based Complementary and Alternative Medicine, 2021*, 1–10.

Yang, N., Shao, H., Deng, J., Yang, Y., Tang, Z., Wu, G., & Liu, Y. (2023). Dictamnine ameliorates chronic itch in DNFB-induced atopic dermatitis mice via inhibiting MrgprA3. *Biochemical Pharmacology, 208*, 115368.

Yao, L., Gu, Y., Jiang, T., & Che, H. (2022). Inhibition effect of PPAR-γ signaling on mast cell-mediated allergic inflammation through down-regulation of PAK1/NF-κB activation. *International Immunopharmacology, 108*, 108692.

Yu, Z., Deng, T., Wang, P., Sun, T., & Xu, Y. (2021). Ameliorative effects of total coumarins from the fructus of *Cnidium monnieri* (L.) Cuss. on 2,4-dinitrochlorobenzene-induced atopic dermatitis in rats. *Phytotherapy Research, 35*(6), 3310–3324.

Zhang, L., Wu, Y., Yang, G., Gan, H., Sang, D., Zhou, J., ... Ma, L. (2020). Design, synthesis and biological evaluation of novel osthole-based derivatives as potential neuroprotective agents. *Bioorganic & Medicinal Chemistry Letters, 30*(24), 127633.

Zhang, Y., Xie, M. L., Xue, J., & Gu, Z. L. (2008). Osthole regulates enzyme protein expression of CYP7A1 and DGAT2 via activation of PPARα/γ in fat milk-induced fatty liver rats. *Journal of Asian Natural Products Research, 10*(8), 797–802.